EUROPEAN ORGANIZATION FOR NUCLEAR RESEARCH

EPS0412
PA-14
PL-11

Measurement of the $\bar{B}^0$ and B^- Meson Lifetimes

The ALEPH Collaboration

Abstract

The lifetimes of the $\bar{B}^0$ and B^- mesons have been measured with the ALEPH detector at LEP, using three different methods. In the first method, semileptonic decays of $\bar{B}^0$ and B^- mesons were partially reconstructed by identifying events containing a lepton with an associated D^{*+} or D^0 meson. The second method used fully reconstructed $\bar{B}^0$ and B^- mesons. The third method, used to measure the $\bar{B}^0$ lifetime, employed a partial reconstruction technique to identify $\bar{B}^0 \to D^{*+}\pi^- X$ decays.

The combined preliminary results are:

$$\begin{aligned} \tau_0 &= 1.54 \pm 0.07 \text{ ps} \\ \tau_- &= 1.58 \pm 0.09 \text{ ps} \\ \frac{\tau_-}{\tau_0} &= 1.02 \pm 0.08 \end{aligned}$$

Contribution to the International Europhysics Conference on High Energy Physics, Brussels, Belgium, July 27 - August 2, 1995

1 Introduction

This paper reports measurements of the $\bar{B}^0$ and B^- lifetimes with the ALEPH detector at LEP using three different techniques. In the first method, which follows closely the analysis of [1], semileptonic decays of $\bar{B}^0$ and B^- mesons were partially reconstructed by identifying events containing a lepton (e or μ) with an associated D^0 or D^{*+} meson. The resulting D^0-lepton ($D^0\ell^-$) and D^{*+}-lepton ($D^{*+}\ell^-$) event samples consist mostly of B^- and $\bar{B}^0$ decays, respectively (charge conjugate modes are implied throughout this paper). The separation of B meson species in this manner allows a measurement of their individual lifetimes. The second method [2] uses $\bar{B}^0$ and B^- mesons reconstructed in exclusive decay modes. The third method uses a partial reconstruction technique to identify $\bar{B}^0$ decays.

2 The ALEPH detector

The ALEPH detector is described in detail elsewhere [3]. A high resolution vertex detector (VDET) consisting of two layers of silicon with double-sided readout is provides precision tracking near the interaction region. It furnishes measurements in the $r\phi$ and z directions at average radii of 6.5 cm and 11.3 cm, with $\simeq$ 12 μm precision. The VDET provides full azimuthal coverage and polar angle coverage to $|\cos\theta| < 0.85$ for the inner layer only and $|\cos\theta| < 0.69$ for both layers [4]. Outside VDET particles traverse the inner tracking chamber (ITC) and the time projection chamber (TPC). The ITC is a cylindrical drift chamber with eight axial wire layers at radii of 16 to 26 cm. The TPC measures up to 21 space points per track at radii between 40 and 171 cm, and also provides up to 338 measurements of the ionization (dE/dx) of each charged track. Tracking is performed in a 1.5 T magnetic field provided by a superconducting solenoid. The combined tracking system yields a momentum resolution of $\sigma(1/p_T) = 0.6 \times 10^{-3}\,(\mathrm{GeV/c})^{-1}$, and the intrinsic impact parameter resolution for high momentum tracks is approximately 25 μm in both the $r\phi$ and z views [5].

The electromagnetic calorimeter (ECAL) is a lead/wire-chamber sandwich operated in proportional mode. The calorimeter is read out in projective towers that subtend typically $0.9^\circ \times 0.9^\circ$ in solid angle and that are segmented in three longitudinal sections. The hadron calorimeter (HCAL) uses the iron return yoke as absorber. Hadronic showers are sampled by 23 planes of streamer tubes, with analog projective tower and digital hit pattern readout. The HCAL is used in combination with two layers of muon chambers outside the magnet for muon identification.

The event samples were selected from approximately 3 million hadronic decays of the Z, collected in the period 1991–1994.

3 Measurements using $D^{(*)}\ell$ correlations

3.1 Event selection

The $D^{*+}\ell^-$ and $D^0\ell^-$ event samples consist of an identified lepton (e or μ) associated with a D^{*+} or D^0 candidate. The selection of muons and electrons is described in detail

in ref. [6]. For this analysis, lepton candidates were required to have a momentum of at least 3 GeV/c.

D^{*+} and D^0 candidates were reconstructed from charged tracks that formed an angle of less than 45° with the lepton candidate. These charged tracks were also required to intersect an imaginary cylinder of radius 2 cm and half-length 4 cm centered on the nominal interaction point, have at least 4 hits in the TPC, have a polar angle θ such that $|\cos\theta| < 0.95$ and have momentum greater than 200 MeV/c.

D^{*+} candidates were identified via the decay $D^{*+} \to D^0\pi^+$, followed by $D^0 \to K^-\pi^+$, $D^0 \to K^-\pi^+\pi^-\pi^+$ or $D^0 \to K^-\pi^+\pi^0$. The difference in mass between the D^{*+} and D^0 candidates was required to lie within 1.5 MeV/c^2 (approximately two standard deviations of the experimental resolution) of the known value of 145.6 MeV/c^2. Since, for these decays, the kaon will have the same electric charge as the lepton coming from the semileptonic decay of the B, this charge correlation was imposed in the reconstruction of D^{*+} mesons. For the subsample where $D^0 \to K^-\pi^+$ the momentum of the D^0 was required to be greater than 5 GeV/c.

The other subsamples suffer from greater combinatorial background and therefore more stringent selection criteria were applied. For the $D^0 \to K^-\pi^+\pi^-\pi^+$ channel: $p_{D^0} >$ 8 GeV/c; if dE/dx information is available for the K track, it must be compatible for that expected of a kaon. At least two of the D^0 decay tracks must have $p > 1$ GeV/c. If, for a given detected lepton, more than one combination satisfied these selection criteria, the best combination was selected, based on the value of the χ^2 of the B vertex fit (discussed below).

For the $D^0 \to K^-\pi^+\pi^0$ channel, π^0 were reconstructed by combining pairs of photons identified in ECAL. The π^0 candidates' momenta were corrected by performing a fit which constrained the candidate mass to the π^0 mass. π^0 candidates with momentum greater than 2 GeV/c were used to form D^0 candidates. The momentum of the D^0 candidates was required to be greater than 10 GeV/c, while the two charged tracks in the decay were required to have at least 0.5 GeV/c of momentum. The same dE/dx criterion was applied for this channel as for the $D^0 \to K^-\pi^+\pi^-\pi^+$ channel above. Futhermore the decay kinematics were required to be consistent with at least one of the three resonant decays:

$$\begin{aligned} D^0 &\to K^-\rho^+ \\ D^0 &\to K^{*-}\pi^+ \\ D^0 &\to \bar{K}^{*0}\pi^0 \end{aligned}$$

For each decay hypothesis the mass of the resonant particle and the cosine of the helicity angle[1] were calculated. If the mass was within 3σ of the known value and the absolute value of the cosine of the helicity angle greater than 0.4, the candidate was considered consistent with the resonant decay hypothesis. In the case of more than one D^0 candidate per identified lepton, the candidate with the best value of $m_{D^0\pi} - m_{D^0}$ was chosen. For this channel it was not possible to use the B vertex χ^2 criterion, as in the $D^0 \to K^-\pi^+\pi^-\pi^+$ case, because here multiple D^0 candidates arise from more than one π^0 candidate with the

[1]The helicity angle is defined as the angle between the scalar particle and one of the decay products of the vector particle calculated in the frame of reference of the vector particle. This angle is distributed as $\cos^2\theta_H$ for the resonant decays listed above.

Table 1: Fitted D^0 mass and number of D^0 candidates and background events falling within a mass window of $\pm 2\sigma$. The uncertainties are statistical only.

Subsample		Mass (MeV/c^2)	Signal events	Background events
$D^{*+}\ell^-$	$D^0 \to K^-\pi^+$	1863.7 ± 0.7	324 ± 19	28 ± 5
	$D^0 \to K^-\pi^+\pi^-\pi^+$	1862.6 ± 0.7	290 ± 18	37 ± 7
	$D^0 \to K^-\pi^+\pi^0$	1862.4 ± 2.7	251 ± 17	31 ± 6
$D^0\ell^-$	$D^0 \to K^-\pi^+$	1863.6 ± 0.5	672 ± 29	113 ± 12

same charged track pair. The B vertex χ^2 is nearly identical for such multiple candidates since it depends almost entirely on the two charged tracks.

The $D^0\ell^-$ sample consists of events with a lepton and a D^0 candidate, where the D^0 was not the decay product of a D^{*+}. D^0 candidates were identified via the decay $D^0 \to K^-\pi^+$. Again, K candidates were required to have the same charge as the lepton. For this sample, the powerful selection criterion involving the D^{*+}–D^0 mass difference was not applicable, making it necessary to apply stricter selection criteria. The D^0 candidates were required to have $p_{D^0} > 8$ GeV/c, $p_K > 2$ GeV/c and $p_\pi > 1.5$ GeV/c. Furthermore, both tracks are required to specific ionization compatible with the particular particle hypothesis. To reject D^0 candidates coming from $D^{*+} \to D^0\pi^+$, a search for the additional pion was performed. If a pion candidate yielding a D^{*+}–D^0 mass difference within 1.5 MeV/c^2 of the known value was found, the $D^0\ell^-$ candidate was rejected. The efficiency for reconstructing the additional pion and rejecting D^0's coming from D^{*+} decays was found to be 85%.

To improve the signal to background ratio and to ensure well-measured decay lengths, additional selection criteria were placed on all the subsamples. The invariant mass of the $D^{(*)}\ell$ (where $D^{(*)}$ can be D^{*+} or D^0) system was required to be greater than 3 GeV/c^2. This criterion significantly reduced the combinatorial background, while keeping $\sim 85\%$ of the signal [7]. To exploit the high precision of the silicon vertex detector, the lepton track and the D^0 decay product tracks were required to have at least one VDET hit in both the $r\phi$ and z projections (except for the decay $D^0 \to K^-\pi^+\pi^-\pi^+$, where at least two of the four tracks were required to have VDET hits). Also, the D and B decay vertices were reconstructed (as will be discussed in Sec. 3.2) and the χ^2 probability for each vertex fit was required to be greater than 1%.

The D^0 candidate mass spectra for the four subsamples are shown in Fig. 1. The fitted curves consist of a Gaussian for the signal plus a linear background. The fitted D^0 mass and the fitted number of signal and background events within a window of $\pm 2\sigma$ around the fitted mass for the three samples are shown in Tab. 1.

3.2 Decay length and proper time

Events reconstructed with a D^0 mass within two standard deviations of the fitted D^0 mass were selected for the lifetime analysis, resulting in 949 $D^{*+}\ell^-$ and 778 $D^0\ell^-$ candidates.

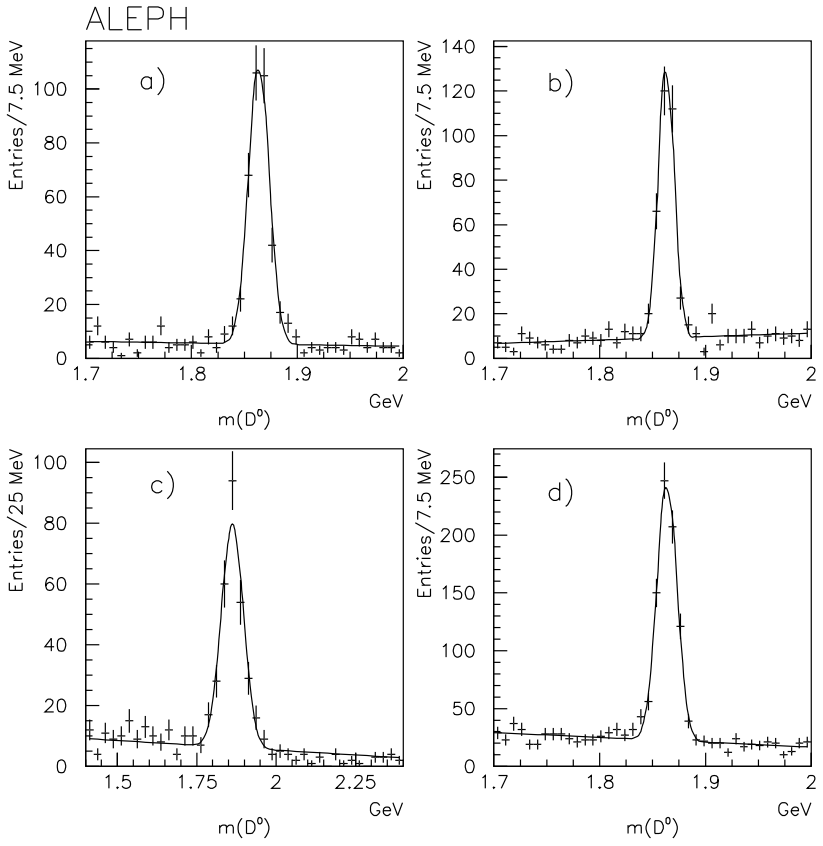

Figure 1: The invariant mass of D^0 candidates for the four subsamples: a) $D^{*+}\ell^-$, $D^0 \to K\pi$, b) $D^{*+}\ell^-$, $D^0 \to K3\pi$, c) $D^{*+}\ell^-$, $D^0 \to K\pi\pi^0$, d) $D^0\ell^-$, $D^0 \to K\pi$. The smooth curves are results of the fit described in the text.

The decay length has been calculated for these events by reconstructing the primary and B decay vertices in three dimensions.

The primary vertex reconstruction algorithm [8], applied to simulated $b\bar{b}$ events, yields an average resolution of $50\mu\text{m} \times 10\mu\text{m} \times 60\mu\text{m}$ (horizontal $\times$ vertical $\times$ beam direction). The B decay vertex was obtained by first reconstructing the D^0 decay vertex using its known decay tracks and then extrapolating the neutral D^0 track backwards where it was combined with the lepton to form the B decay vertex. For the $D^0 \to K^-\pi^+\pi^0$ channel, the D^0 vertex was constructed using only the charged tracks, but the π^0 momentum was included when extrapolating the neutral D^0 track backwards to form the B vertex. In the case of $D^{*+}\ell^-$ events, the soft pion from the D^{*+} decay does not improve the resolution on the B decay length and was therefore not used in the reconstruction of the B vertex.

The best estimates of the B decay length and its error were obtained by projecting the distance between the primary and B decay vertices onto the direction defined by the $D^{(*)}\ell$ system. The uncertainty on the flight direction due to the missing neutrino induces a negligible error on the decay length. The resolution on the B decay length is typically about 300 μm, compared with an average B decay length of ~ 2.5 mm.

The B momentum is reconstructed using an energy flow technique as described in [9].

The momentum resolution obtained using this technique is between 8 and 10%, depending on the decay channel.

3.3 $\bar{B}^0$ and B^- lifetimes

Both the $D^{*+}\ell^-$ and $D^0\ell^-$ samples contain a mixture of $\bar{B}^0$ and B^- decays and the $B^-/\bar{B}^0$ mixture in the samples depends on the ratio of the lifetimes, as will be discussed below. Therefore, to measure the $\bar{B}^0$ and B^- lifetimes a simultaneous maximum likelihood fit to all the events was performed. The likelihood function contains three components for each sample and is written as:

$$\begin{aligned}\mathcal{L}_0 &= \prod_{i=1}^{N_{D^*\ell}} f_-^* F(t_i,\sigma_i,\tau_-) + f_0^* F(t_i,\sigma_i,\tau_0) + f_{BG}^* F_{BG}^*(t_i) \\ &\times \prod_{i=1}^{N_{D^0\ell}} f_-^0 F(t_i,\sigma_i,\tau_-) + f_0^0 F(t_i,\sigma_i,\tau_0) + f_{BG}^0 F_{BG}^0(t_i) \qquad (1)\end{aligned}$$

where $F(t,\sigma,\tau)$ is the probability function for the signal, which consists of an exponential function convolved with momentum and decay length resolution functions. The coefficients f_-^* and f_0^* are the fractions of the $D^{*+}\ell^-$ sample arising from B^- and $\bar{B}^0$ decays, respectively. Similarly, f_-^0 and f_0^0 are the fractions of the $D^0\ell^-$ sample made up of B^- and $\bar{B}^0$ decays. The coefficients f_{BG}^* and f_{BG}^0 are the background fractions of the samples, while the functions $F_{BG}^*(t)$ and $F_{BG}^0(t)$ are their normalised proper time distributions.

3.3.1 Backgrounds

Background contamination arises from the following sources:

(1) combinatorial background, i.e. candidates with a fake $D^{(*)}$;

(2) the process $\bar{B} \to D_s^- D^{(*)} X$, followed by $D_s^- \to \ell^- X$, giving rise to a real $D^{(*)}$ and a real lepton;

(3) a real $D^{(*)}$ meson accompanied by a fake or non-prompt lepton, from $Z \to b\bar{b}$ or $Z \to c\bar{c}$ events.

Source (1) is the dominant background and its contribution is determined from a fit to the D^0 mass distributions, and its magnitude is given in Tab. 1 for the various subsamples. The proper time distribution for this source has been determined from the data by selecting events from the sidebands of the D^0 peak. The same selection criteria described in Sec. 3.1 have been applied to the background samples, except that the requirement on the D^{*+}–D^0 mass difference in the case of the $D^{*+}\ell^-$ events has been removed to increase the statistics. A function consisting of a Gaussian plus positive and negative exponential tails was used to describe these data.

The contribution from source (2) was calculated from the measured branching ratios for this process [10] plus a Monte Carlo simulation to determine the detection efficiency. This background made up 2–3% of the samples, depending on the channel.

The background from source (3) is estimated from the measured hadron-lepton misidentification probabilities [6] and the measured inclusive D^0 and D^{*+} rates. An independent estimate was made using wrong-sign ($D^{*+}\ell^+$ or $D^0\ell^+$) events. This background source contributes $3 \pm 1.5\%$ to the samples. The proper time distribution for sources (2) and (3) were determined using simulated events.

3.3.2 Sample compositions

The sample compositions (the coefficients f_-^*, f_0^*, $f_-^0$and f_0^0 of Eq. 1) must be calculated to complete the specification of the likelihood function. The difficulty in evaluating the sample compositions arises from incomplete knowledge of the branching ratios of certain decay modes that contribute to the two samples.

The $\bar{B}^0$ and B^- content of the two samples were calculated using the following method: the relevant semileptonic branching ratios for $\bar{B}^0$ mesons were taken from measurements at the $\Upsilon(4S)$ energy. Where measurements were incomplete, isospin conservation was applied, as well as the constraint that the sum of the exclusive channels equal the inclusive $\bar{B}^0$ semileptonic branching ratio. The B^- branching fractions were then obtained from

$$B(B^- \to \ell^- X) = \frac{\tau_-}{\tau_0} B(\bar{B}^0 \to \ell^- X') \qquad (2)$$

which derives from the expectation that the partial semileptonic decay widths are equal. The sample coefficients were then calculated by considering the $\bar{B}^0$ and B^- decay channels that contribute to the $D^{*+}\ell^-$ and $D^0\ell^-$ samples. As a consequence of this procedure, the coefficients f_-^*, f_0^*, f_-^0 and f_0^0 appearing in the likelihood function (Eq. 1) depend on the lifetime ratio. The full calculation [11] shows that, for equal lifetimes, one obtains $87 \pm 4\%$ of the B decays in the $D^{*+}\ell^-$ sample are attributed to $\bar{B}^0$, while $75 \pm 5\%$ of the $D^0\ell^-$ sample B decays come from B^-.

3.3.3 Fit results

A maximum likelihood fit to the proper time distributions of the $D^{*+}\ell^-$ and $D^0\ell^-$ events was performed to determine the two free parameters τ_0 and τ_-. The values obtained are

$$\begin{aligned} \tau_0 &= 1.61 \pm 0.07 \text{ ps} \\ \tau_- &= 1.58 \pm 0.08 \text{ ps} \end{aligned}$$

where the errors are statistical only. The correlation coefficient is -0.35. The ratio of the lifetimes is:

$$\frac{\tau_-}{\tau_0} = 0.98 \pm 0.08,$$

taking into account the correlation between the lifetimes.

The proper time distributions for the two samples are shown in Fig. 2, with the results of the fit overlaid.

As a check on the procedure, a measurement of the D^0 lifetime has been performed. The D^0 flight distance is calculated as the distance between the B and D^0 decay vertices, projected onto the D^0 direction. An unbinned likelihood fit to the 1727 events yields

$$\tau_{D^0} = 0.404 \pm 0.012 \text{ (stat) ps}$$

in agreement with the world average value $\tau_{D^0} = 0.415 \pm 0.004$ ps [12].

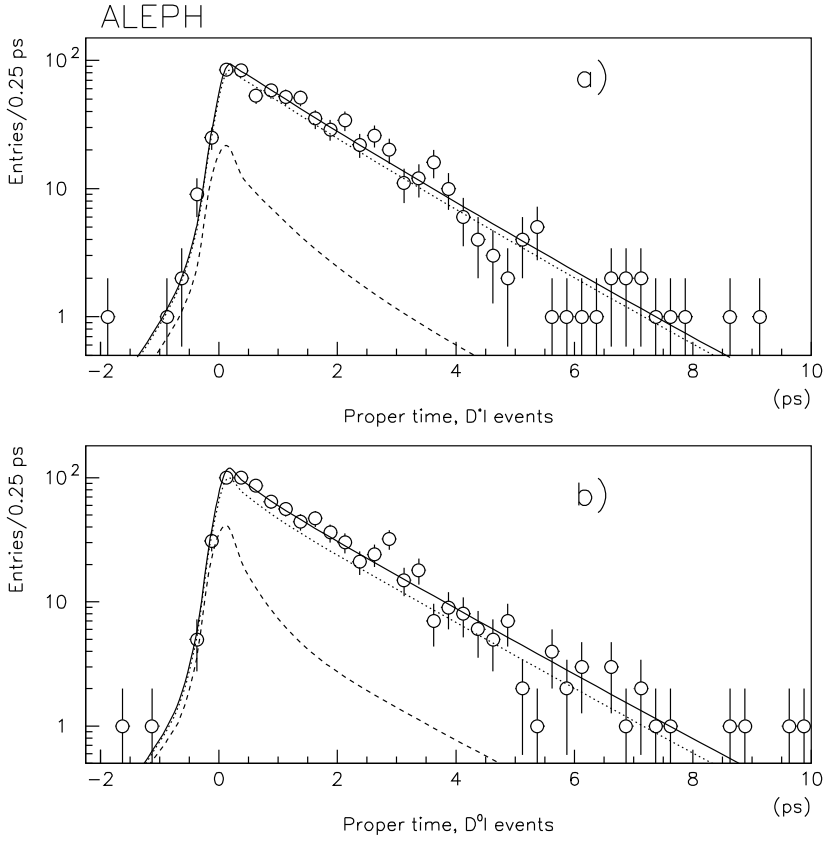

Figure 2: Proper time distributions with result of the fit overlaid for the two samples. a) $D^{*+}\ell^-$ events; the dotted line is the background contribution to the fit, while the dashed line is the sum of the background and $\bar{B}^0$ components; b) $D^0\ell^-$ events, the dotted line is the background contribution to the fit, while the dashed line is the sum of the background and B^- components.

3.3.4 Systematic uncertainties

Several sources of systematic error have been considered.

The systematic uncertainty due to the sample compositions was determined by varying the branching fractions of Table 2 within their errors.

Uncertainties in the background fractions and proper time distributions have been considered. Different background samples have been selected by varying the sideband regions and by using events with wrong-sign correlations, and alternative parametrizations of the proper time distributions have been studied.

The uncertainty in the B momentum reconstruction comes mainly from the uncertainty in the D^{**} content of semileptonic B decays. There is approximately a 2% error in the B momentum determination [9].

Although the sample compositions are independent of the nominal reconstruction ef-

Table 2: B branching fractions used in the lifetime measurement.

Decay	Branching ratio (%)	Reference
$\bar{B}^0 \to D^{*+}\ell^-\nu$	4.50 ± 0.45	[13, 14]
$\bar{B}^0 \to D^{+}\ell^-\nu$	1.9 ± 0.5	[12]
$B^- \to D^{*+}\pi^-\ell^-\nu$	0.96 ± 0.33	[15]
$\bar{B}^0 \to \ell^- X$	10.4 ± 1.1	[13, 16]

Table 3: Sources of systematic error on the fitted lifetimes.

Source of error	Contribution to systematic error		
	τ_0 (ps)	τ_- (ps)	τ_-/τ_0
Sample compositions	± 0.013	± 0.018	± 0.015
Background treatment	± 0.023	± 0.021	± 0.010
B momentum reconstruction	$^{+0.030}_{-0.027}$	$^{+0.030}_{-0.027}$	± 0.010
$D^{(*)}\pi\ell^-\nu$ relative efficiency	± 0.008	± 0.007	± 0.008
Decay length resolution	± 0.010	± 0.010	± 0.010
Total	$^{+0.042}_{-0.040}$	$^{+0.043}_{-0.041}$	± 0.024

ficiencies, the relative efficiencies

$$\epsilon^{**} = \frac{\epsilon(B \to D^{(*)}\pi\ell\nu)}{\epsilon(B \to D^{(*)}\ell\nu)}$$

enter into the calculation and this uncertainty has been propagated to the systematic error on the lifetimes.

The uncertainty due to the decay length resolution function was estimated by allowing a variation of its parameters consistent with their statistical errors plus a systematic error due to uncertainty in the Monte Carlo model of the decay length resolution.

The various contributions to the systematic error are presented in Table 3.

4 Measurements using fully reconstructed candidates

4.1 Event selection

The B^+ candidates were reconstructed using the following decays:

$B^+ \longrightarrow \bar{D}^0\pi^+$
$\quad\quad \hookrightarrow K^+\pi^-$, $K^+\pi^-\pi^0$, $K^+\pi^-\pi^+\pi^-$, $K^0_S\pi^+\pi^-$

$B^+ \longrightarrow \bar{D}^0 \; a_1^+$
  $\quad\quad\quad\quad \hookrightarrow \pi^+\pi^+\pi^-$ (from a_1^+)
  $\quad\quad \hookrightarrow K^+\pi^-, \; K_S^0\pi^+\pi^-$ (from $\bar{D}^0$)

$B^+ \longrightarrow J/\psi \; K^+$

$B^+ \longrightarrow \psi(2S) \; K^+$
  $\quad\quad \hookrightarrow J/\psi \; \pi^+\pi^-, \; e^+e^-, \; \mu^+\mu^-$

$B^+ \longrightarrow (J/\psi, \; \psi(2S)) \; K^{*+}$
  $\quad\quad\quad\quad \hookrightarrow K_S^0\pi^+$
  $\quad\quad \hookrightarrow e^+e^-, \; \mu^+\mu^-$

and the following decays were used to reconstruct the B^0 candidates:

$B^0 \longrightarrow D^-\pi^+$
  $\quad\quad \hookrightarrow K^+\pi^-\pi^-$

$B^0 \longrightarrow D^{*-}\pi^+$
  $\quad\quad \hookrightarrow \bar{D}^0\pi^-$
  $\quad\quad\quad \hookrightarrow K^+\pi^-, \; K^+\pi^-\pi^0, \; K^+\pi^-\pi^+\pi^-, \; K_S^0\pi^+\pi^-$

$B^0 \longrightarrow D^{*-} \; \rho^+$
  $\quad\quad\quad\quad \hookrightarrow \pi^+\pi^0$ (from ρ^+)
  $\quad\quad \hookrightarrow \bar{D}^0\pi^-$ (from D^{*-})
  $\quad\quad\quad \hookrightarrow K^+\pi^-, \; K^+\pi^-\pi^+\pi^-, \; K_S^0\pi^+\pi^-$

$B^0 \longrightarrow D^{*-} \; a_1^+$
  $\quad\quad\quad\quad \hookrightarrow \pi^+\pi^+\pi^-$ (from a_1^+)
  $\quad\quad \hookrightarrow \bar{D}^0\pi^-$ (from D^{*-})
  $\quad\quad\quad \hookrightarrow K^+\pi^-, \; K^+\pi^-\pi^0, \; K_S^0\pi^+\pi^-$

$B^0 \longrightarrow J/\psi \; K_S^0$

$B^0 \longrightarrow \psi(2S) \; K_S^0$
  $\quad\quad \hookrightarrow J/\psi \; \pi^+\pi^-, \; e^+e^-, \; \mu^+\mu^-$

$B^0 \longrightarrow (J/\psi, \; \psi(2S)) \; K^{*0}$
  $\quad\quad\quad\quad \hookrightarrow K^+\pi^-$
  $\quad\quad \hookrightarrow e^+e^-, \; \mu^+\mu^-$

In each event, only one B candidate was selected within a mass window of ± 1 GeV/c^2 of the B meson mass, using the best B vertex probability candidate.

Muons were selected using HCAL and muon chambers after a cut at 2.5 GeV/c in momentum. Electrons were selected with momenta greater than 1 GeV/c using dE/dx information and ECAL estimators. Electron candidates were checked not to come from photon conversions. Charged pions were selected using all charged tracks, rejecting only

tracks which have dE/dx information available and $|R_I(\pi)| > 3$. Charged kaons had to have momenta greater than 2 GeV/c and dE/dx information available and compatible with the kaon hypothesis. Muon candidates were not considered as kaon candidates. Neutral pions were reconstructed using the decay $\pi^0 \to \gamma\gamma$. Neutral kaons were reconstructed using the decay $K^0_S \to \pi^+\pi^-$. J/ψ mesons were reconstructed in the e^+e^- and $\mu^+\mu^-$ channels.

The $D^0 \to K^-\pi^+\pi^0$ candidates were selected using the following mass hypotheses: $K^-\rho^+$, $K^{*-}\pi^+$ and $\bar{K}^{*0}\pi^0$. For the $D^0 \to K^-\pi^+\pi^+\pi^-$ channel, the mass hypotheses were $K^-\pi^+\rho^0$, $\bar{K}^{*0}\pi^+\pi^-$ and $\bar{K}^{*0}\rho^0$. The $D^0 \to K^0_S\pi^+\pi^-$ candidates had to be either $K^{*-}\pi^+$ or $K^{*+}\pi^-$, which was necessary to know the nature of the D meson (either a D^0 or a $\bar{D}^0$).

The mass windows to select the D mesons candidates were between ± 15 MeV/c^2 and ± 30 MeV/c^2 depending on the channels, and the minimum momenta required varied between 4 GeV/c and 9 GeV/c. D^{*+} candidates were selected if the difference between their mass and the corresponding D^0 candidate mass was between 143.4 MeV/c^2 and 147.4 MeV/c^2.

To reconstruct the $B \to DX$ channels, minimum cuts were applied on the X particle momentum (p_X) and the B candidate energy ($X_B = E_B/E_{beam}$). These cuts were between 5 GeV/c and 9 GeV/c for p_X, depending on the channels, and between 0.50 and 0.70 for X_B. Cuts were also applied on $\cos\theta^*$, where θ^* is the angle between the D meson direction in the B rest frame and the B meson flight direction, for two channels. These cuts were: $-0.7 < \cos\theta^* < 0.4$ for $B^+ \to \bar{D}^0 a_1^+$ and $\cos\theta^* > -0.5$ for $B^0 \to D^-\pi^+$.

The mass windows to select the ψ candidates were ± 100 MeV/c^2 for J/ψ or $\psi(2S) \to \ell^+\ell^-$ and ± 200 MeV/c^2 for $\psi(2S) \to J/\psi\pi^+\pi^-$. For this last channel a cut was applied on the $\pi^+\pi^-$ mass, requiring it to be greater than 0.4 GeV/c^2.

In the $B^+ \to \bar{D}^0 X^+$ channels, the D^0 candidate was accepted only if no good D^{*+} could be reconstructed with this D^0. Events compatible with $D_s^+ \to K^-K^+\pi^+$ and $\Lambda_c^+ \to K^-p\pi^+$ were rejected in the $D^+ \to K^-\pi^+\pi^+$ selection if the mass of the three final state particles (using the D_s^+ or Λ_c^+ hypotheses) was within 25 MeV/c^2 of the D_s^+ or Λ_c^+ masses. These hypotheses were tested successively for the two pion candidates except for those which have dE/dx information available. If dE/dx was available, the mass test was only made if the pion candidate was compatible with a kaon (for D_s^+) or a proton (for Λ_c^+) hypothesis. Semileptonic decays were also rejected requiring the pion candidates in the $B \to D(n\pi)$ and $D \to K(n\pi)$ decays to be inconsistent with electron or muon hypotheses.

For each B decay vertex in the $B \to \psi X$ channels and each D decay vertex in the $B \to DX$ channels (see figure 3), at least two tracks had to have vertex detector hits (at least one hit in the $r-\phi$ side and one hit in the z side of the same layer). In the $B \to DX$ channels, for each B decay vertex, at least one track was required to have vertex detector hits in addition to the D "track" from the vertex fitting procedure. The minimum cut on the χ^2 probability of each secondary vertex was 0.5%.

4.2 B^+ and B^0 signal

The mass spectra of the candidates obtained after all the selection cuts are shown in Figure 4. A total of 94 B^+ and 121 B^0 candidates were selected within a mass window

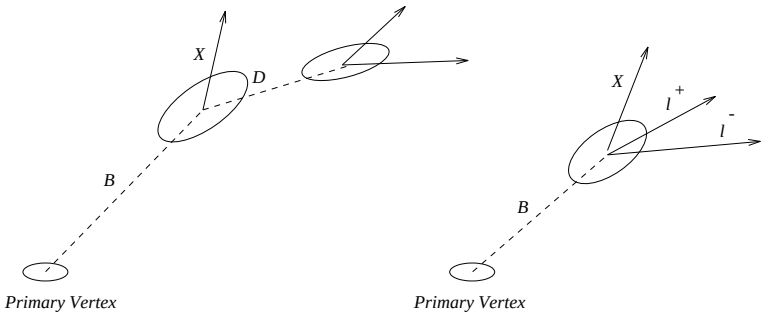

Figure 3: Decay topologies for $B \to DX$ and $B \to \psi X$ channels.

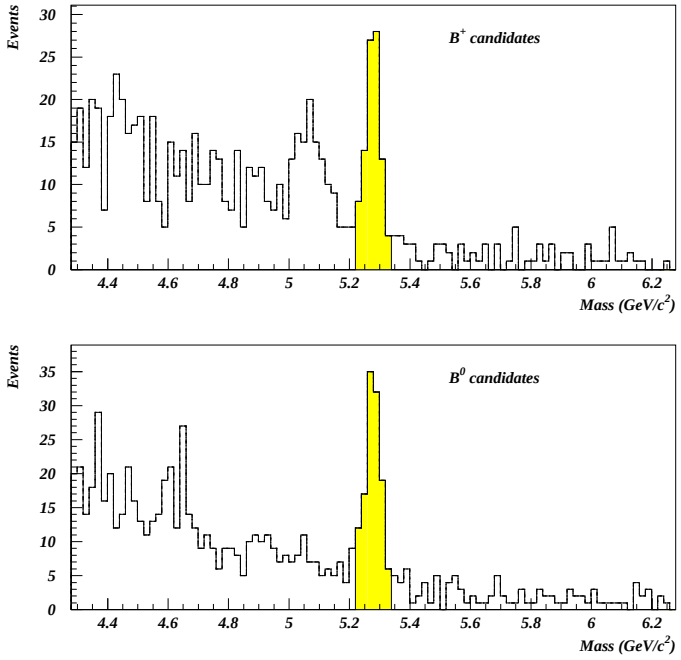

Figure 4: Mass spectra of the B^+ and B^0 candidates reconstructed using 1991, 1992, 1993 and 1994 events. Candidates selected for the lifetime measurement are shaded.

of ± 60 MeV/c^2 around the B meson mass (5.279 GeV/c^2) for the lifetime measurement.

Most of the signal candidates in the samples selected for the lifetime measurement were fully reconstructed but some of them were mis-reconstructed using particles from fragmentation. These mis-reconstructed signal candidates (about 10% of the signal) have correct decay lengths. However, mis-reconstruction degrades the measurement of the boost, the resolution being about 1% for half of these events and around 20% for the remaining half. These mis-reconstructed candidates can be separated into two components. The first component (called "corrupted signal") contains candidates which were reconstructed losing a soft photon or using neutral particles from fragmentation or using a low momentum fragmentation track so that their selection efficiency does not depend on their proper time. The proper time distribution of the candidates found in a $b\bar{b}$ sim-

ulation was fitted with an exponential yielding a lifetime in good agreement with the generated lifetime. These candidates were taken as signal in the final fit. The second component (called "wrong signal") contains candidates which were reconstructed using one high momentum or a few charged particles from fragmentation. These candidates can only be reconstructed if their decay length is very short, to allow charged particles from the primary vertex to be associated with their decay vertex, leading to a selection efficiency which decreases quickly at high decay length. The proper time distribution of these candidates found in a $b\bar{b}$ simulation has been fitted, yielding a lifetime of $0.31^{+0.13}_{-0.09}$ ps for this sample which represents 3.4% of the B^+ signal sample and 5.6% of the B^0 signal sample (separate fits to the distributions of B^+ and B^0 samples give results in perfect agreement). This small low lifetime component was taken into account in the final fit. The selected samples contain also a small contamination from other B hadrons which represents about 2% of the signal. This contamination was taken into account in the systematic errors. Finally, the samples selected for the lifetime measurement contain combinatorial background candidates originating from non-$b\bar{b}$ events with zero lifetime and a small component of background events with non-zero lifetime from $c\bar{c}$ events and $b\bar{b}$ events.

The peak around 5-5.1 GeV/c^2 in the B^+ mass spectrum is reproduced in the simulation. This effect is mainly due to $B^+ \rightarrow \bar{D}^{*0}(\rightarrow \bar{D}^0\pi^0)X^+$ reconstructed as $B^+ \rightarrow \bar{D}^0X^+$, losing the soft π^0. But there are also a few $B^0 \rightarrow D^{*-}(\rightarrow \bar{D}^0\pi^-)X^+$ mesons reconstructed as "B^+"$\rightarrow \bar{D}^0X^+$ losing the soft π^-.

4.3 Lifetime extraction

The proper time (t) of each candidate was calculated from the reconstructed decay length (l), mass (m) and momentum (p) as: $t = \frac{lm}{p}$. The decay length l was obtained by projecting the vector joining the interaction point and the B decay vertex onto the B flight direction taken as its momentum direction. The position of the B decay vertex was reconstructed in three dimensions by vertexing the charged tracks from the secondary vertices. The error on the proper time was calculated for each candidate using the error on the reconstructed decay length calculated event by event and the correction factor S applied to this error in order to take into account the under-estimation of this error. The mean relative boost error was extracted from simulated samples and was found to be between 0.3% and 0.9% for the various channels.

The background lifetime was studied in the data using three background samples. For the $B \rightarrow DX$ channels, the wrong sign candidates were constructed as, for example, $D^{*-}X^-$, $D^-\pi^-$ or D^0X^+ (the nature of the neutral D candidate was determined by the charge of its kaon daughter). For the $B \rightarrow \psi X$ channels, the wrong sign candidates were constructed using "ψ"$\rightarrow \ell^\pm\ell^\pm$. The side band candidates were constructed combining fake D or ψ candidates extracted from their mass spectrum side bands. These fake D candidates were selected around 2.0 GeV/c^2, the difference between the D^{*+} and the D^0 candidates being required to be around 200 MeV/c^2, with the same mass windows. The fake J/ψ were selected between 2.4 GeV/c^2 and 2.8 GeV/c^2 whereas the fake $\psi(2S)$ were selected between 3.2 GeV/c^2 and 3.5 GeV/c^2. The "wrong sign side band" candidates were constructed combining the previous two techniques.

The distribution of the reconstructed decay length divided by its computed error

for candidates from these background samples (with a mass between 4.3 GeV/c^2 and 6.3 GeV/c^2) was fitted with a gaussian plus an exponential. This fitted gaussian was used to measure a resolution correction factor S in the data, the result of the fit being $S = 1.27 \pm 0.03$.

The fraction of background with non-zero lifetime (f_{exp}) and its lifetime (τ_{exp}) were measured in the data using these three background samples, separately for the $B \to DX$ and $B \to \psi X$ channels. The proper time distribution of the $B \to \psi X$ background candidates from "signal" and the three background samples between 5.4 GeV/c^2 and 6.3 GeV/c^2 merged was fitted with a gaussian centered at zero plus an exponential convolved with a gaussian, the result of this fit is: $f_{exp} = 50 \pm 11\%$ and $\tau_{exp} = 0.72 \pm 0.03$ ps. The proper time distribution of the $B \to DX$ background candidates from the three background samples between 5.4 GeV/c^2 and 6.3 GeV/c^2 merged was fitted with the previous background proper time function. Using the value for τ_{exp} from $B \to \psi X$ channels, the result of the fit is $f_{exp} = 3.9 \pm 1.5\%$, since this non-zero lifetime fraction is so small a fit with both τ_{exp} and f_{exp} free does not converge in this channel.

The proper time distribution of the B^+ and B^0 samples were fitted separately by maximizing an unbinned likelihood function simultaneously on the $B \to DX$ and $B \to \psi X$ samples, with two different background fractions f^D_{bkg} and f^ψ_{bkg}. The signal proper time distribution is an exponential convolved with a gaussian (plus another one with a lifetime of 0.31 ps to take into account the presence of B mesons partially reconstructed with fragmentation tracks). The background proper time distribution was a gaussian centered at zero plus an exponential convolved with a gaussian with a lifetime of τ_{exp}. There are only three free parameters in the fit: the two background fractions f^D_{bkg} and f^ψ_{bkg}, and the signal lifetime τ_B.

4.4 Results

The fitted lifetime of the 94 B^+ candidates is:

$$\tau_- = 1.58^{+0.21}_{-0.18} \text{ ps}$$

with $f^D_{bkg} = 13.1^{+5.7}_{-5.0}\%$ and $f^\psi_{bkg} = 9.3^{+21.4}_{-15.2}\%$. For the 121 B^0 candidates, the fitted lifetime is:

$$\tau_0 = 1.25^{+0.15}_{-0.13} \text{ ps}$$

with $f^D_{bkg} = 17.4^{+5.8}_{-5.4}\%$ and $f^\psi_{bkg} = 1.0^{+21.9}_{-13.0}\%$. The proper time distributions together with the fit results are shown in figure 5. Fitting simultaneously the two distributions yields:

$$\frac{\tau_-}{\tau_0} = 1.27^{+0.23}_{-0.19}$$

Systematic errors from various sources were estimated and are summarized in table 4.

The uncertainty on the background lifetime was estimated separately for the $B \to DX$ and $B \to \psi X$ channels. In the $B \to DX$ channels, f_{exp} was varied from 0 to 15.6% (which is four times the nominal value). The proper time distribution was also replaced by two gaussians instead of one gaussian plus an exponential. In the $B \to \psi X$ channels, f_{exp} has been varied from 0 to 75% (which is 50% more than the nominal value).

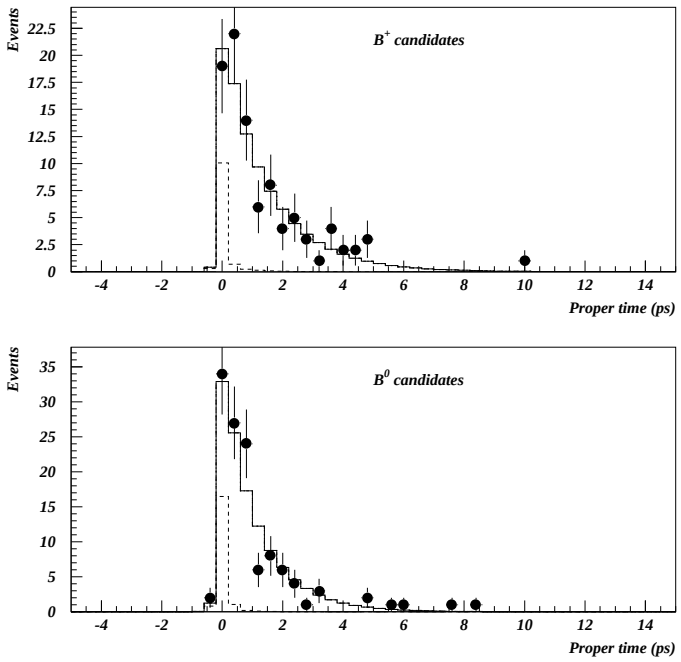

Figure 5: B^+ and B^0 proper time distributions fitted (solid line). The dashed line represents the background component, a gaussian centered at zero and an exponential.

The correction factor S has been varied between 1.0 and 1.5, the nominal value measured in the data being 1.27. Doubling the boost resolution does not change significantly the fit results.

It was mentioned in section 4.2 that about 5% of the signal has a worse boost resolution (corrupted signal) and taking this effect into account decreases slightly the fitted lifetime by an amount taken as asymmetric systematic error. Also, the fraction of the exponential with a lifetime of 0.31 ps in the signal distribution has been varied by $\pm 100\%$ (from 0 to 6.8% for the B^+ sample and from 0 to 11.2% for the B^0 sample) to estimate the systematic error from this wrong signal.

It was shown in section 4.2 that there is a small contamination from other B hadrons in the signal samples. The effects of the contamination by B^0 mesons in the B^+ sample and by B^+, B_s^0 and Λ_b^0 hadrons in the B^0 sample were estimated using the fitted B^+ and B^0 lifetimes and the B_s^0 and Λ_b^0 average lifetimes corrected by the use of the wrong mass when taken as B^0 candidates.

Since the background fractions were left free in the fit, the uncertainty from this was included in the statistical error. Table 4 summarizes the various systematic errors, total errors being ± 0.04 ps for the B^+ lifetime and ± 0.05 ps for the B^0 lifetime.

As a check, the selection cuts were applied on a high statistics dedicated simulation (corresponding to about 20 million Z for the B^+ sample and 100 million Z for the B^0 sample). The fitted lifetimes of these signal candidates are in perfect agreement with the generated lifetime. This result excludes any bias in the reconstructed proper time distri-

Table 4: List of systematic errors.

Error	τ_{B^+}	τ_{B^0}	τ_{B^+}/τ_{B^0}
$B \to DX$ background	$^{+0.014}_{-0.007}$ ps	$^{+0.016}_{-0.010}$ ps	$^{+0.002}_{-0.006}$
$B \to \psi X$ background	$^{+0.015}_{-0.011}$ ps	± 0.001 ps	$^{+0.010}_{-0.009}$
Correction factor S	$^{+0.001}_{-0.002}$ ps	$^{+0.002}_{-0.001}$ ps	$^{+0.001}_{-0.004}$
Wrong and corrupted signal	± 0.031 ps	$^{+0.044}_{-0.042}$ ps	$^{+0.020}_{-0.021}$
Contamination	$+0.014$ ps	$^{+0.001}_{-0.013}$ ps	$^{+0.024}_{-0.001}$
Total	± 0.04 ps	± 0.05 ps	± 0.03

bution from the selection cuts. The proper time distribution of the candidates selected on a simulated sample of 3.7 million $q\bar{q}$ events was also fitted taking into account the background. The result of this fit is also in agreement with the generated lifetime.

As a consistency check, the D meson lifetimes were also measured using the $B \to DX$ candidate events. The 29 $B^0 \to D^- \pi^+$ candidates were used to measure the D^+ lifetime giving $\tau_{D^+} = 1.17^{+0.25}_{-0.19}$ ps in agreement with the world average of $\tau_{D^+} = 1.057 \pm 0.015$ ps. The D^0 lifetime was also measured using the 154 $B^+ \to \bar{D}^0 X^+$ and $B^0 \to D^{*-}(\to \bar{D}^0 \pi^-) X^+$ candidates. The result of the fit is $\tau_{D^0} = 0.407^{+0.038}_{-0.034}$ ps in agreement with the world average of $\tau_{D^0} = 0.415 \pm 0.004$ ps.

5 Measurement using partially reconstructed hadronic B^0 decays

To increase the reconstruction efficiency for hadronic B^0 decays

$$\begin{array}{rcl} B^0 \;\to\; \pi_B^+ \;\; X \;\; D^{*-} & & \\ \qquad\qquad\quad \hookrightarrow \pi_D^- \overline{D}^0 & & \end{array} \tag{3}$$

a partial reconstruction technique was used. The D^{*-} momentum can be approximated from the π_D^- momentum with a precision of about 15% due to the small momentum transfer in the D^{*-} decay. This is not good enough to distinguish between two body decays like $B^0 \to \pi^+ D^{*-}$ and $B^0 \to \rho^+ D^{*-}$ with a missing π^0 from the ρ^+ decay. But it allows an inclusive reconstruction of decays of the type (3) from the two pions $\pi_B^+ \pi_D^-$ if the system X has low momentum and mass. The problem of approximating the B^0 three-momentum from the π_B^+ and π_D^- momenta can be solved in the $\pi_B^+ \pi_D^-$ rest frame. Assuming a given $D^0 X$ mass the B^0 energy in this frame is given by:

$$E_B^* = \frac{M_B^2 + M_{\pi_B \pi_D}^2 - M_{XD^0}^2}{2 M_{\pi_B \pi_D}} \tag{4}$$

The XD^0 mass was set to $M_{XD^0} = 2.1$ GeV/c^2 which gives the best momentum direction resolution (12 mrad in the laboratory frame) for a mixture of $B^0 \to \pi^+(\rho^+)D^{*+}$ decays, the two decay modes for which the selection was optimized. For decays where the true missing mass is close to this value, the B^0 flight direction is approximately the direction of the slow pion:

$$\vec{p}_B^{\,*} \approx \sqrt{(E_B^*)^2 - M_B^2} \cdot \frac{\vec{p}^{\,*}_{\pi_D}}{|\vec{p}^{\,*}_{\pi_D}|} \tag{5}$$

The B^0 momentum in the laboratory frame is obtained after a retransformation from the $\pi_B^+\pi_D^-$ rest frame to the laboratory frame. The momentum resolution is 2 GeV/c for $B^0 \to \pi^+(\rho^+)D^{*+}$ decays and 8 GeV/c for the remaining decays contributing to the signal.

The calculation of the B momentum implicitly requires $M_{\pi\pi} < M_B - M_{XD^0} \approx 3.2$ GeV/c^2, while the kinematic limit for pions from reaction (3) is $M_{\pi_B\pi_D} < 1.5$ GeV/c^2. Reconstructed B^0 mesons are identified as an excess in the $\pi_B^+\pi_D^-$ mass distribution below 1.5 GeV/c^2.

5.1 Data selection

Oppositely charged pion pairs $\pi_B^+\pi_D^-$, consistent with coming from a common vertex within 3 standard deviations, were selected. The B^0 momentum $\vec{p}_B$ was determined using the technique described above. Selecting events with high B^0 momenta 30 GeV/c $< |\vec{p}_B| <$ 45 GeV/c and a B^0 decay angle $|\cos\theta^*_{B,\pi_B^+}| < 0.8$ suppressed background and improved the determination of the B^0 flight direction. The B^0 flight direction and decay length $\vec{\ell}_B$ was measured directly from the primary and secondary $\pi_B^+\pi_D^-$ vertex: $\vec{\ell}_B = \vec{r}_{\pi\pi} - \vec{r}_{primary}$. To improve the resolution, this measurement was combined with the jet direction using a χ^2 minimization. Jets were built using the JADE cluster algorithm [17] with a y_{cut} of 0.008. The value of y_{cut} was optimized to get the best approximation of the B^0 flight direction from the jet direction. The resolution is about 20 mrad. The B^0 flight direction was determined independently from the B^0 decay length $\vec{\ell}_B$ and from the B^0 momentum. The angle between $\vec{\ell}_B$ and $\vec{p}_B$ was required to be less than 25 mrad.

Background candidates from $B^+ \to \pi^+\pi^+XD^{*-}$ decays were identified and rejected. These candidates were selected by requiring an additional π^+ coming from the secondary $\pi_B^+\pi_D^-$ vertex. The B^+ momentum can be approximated from equation (5), replacing M_{XD^0} with M_{D^0} and the two pion mass with the three pion mass in formula (4). The angle between the B^+ momentum and the flight direction had to be smaller than 20 mrad. Excluding these events rejected 60 % of $B^+ \to \pi^+\pi^+XD^{*-}$ decays while only 20% of the B^0 decays were lost.

The B^0 lifetime was measured from candidates with a proper decay time

$$20 \text{ ps} > t = \frac{|\vec{\ell}_B| \cdot M_B}{|\vec{p}_B| \cdot c} > 1 \text{ ps}$$

At small decay lengths background from light quark production is dominant. The resolution of the decay time is dominated by the error on the decay length. The resolution function R^ℓ can be described by a sum of three gaussians with widths of 260μm, 780μm

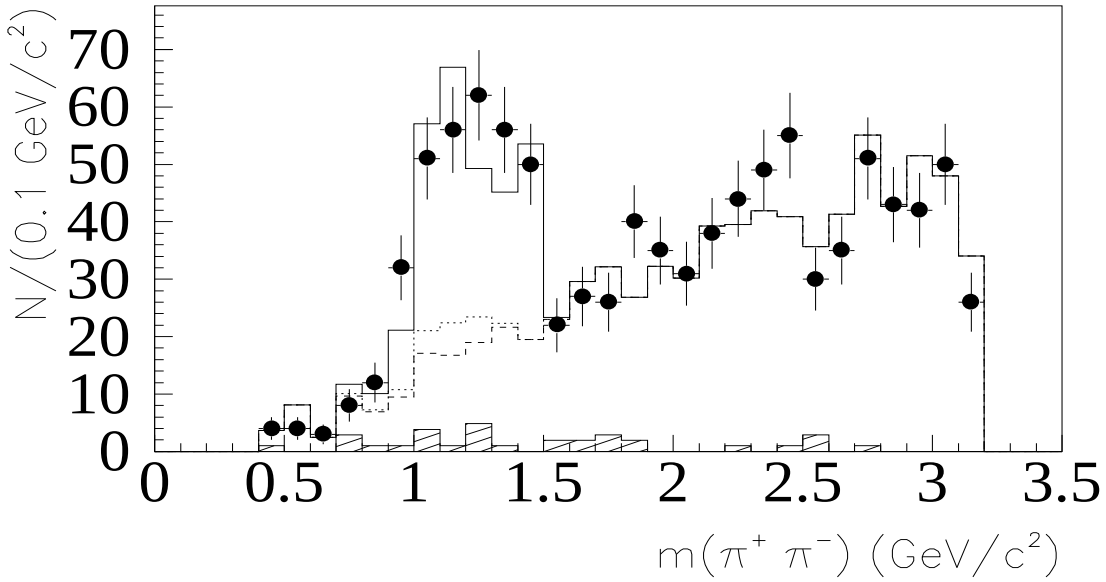

Figure 6: $\pi_B^+\pi_D^-$ mass distributions. Shown are the data (with error bars) and the Monte Carlo simulation (histograms). The contributions from light quark background (hatched), $b\bar{b}$ background (dashed), $B^+ \to \pi_B^+ X D^{*-}$ (dotted) and the $B^0 \to \pi_B^+ X D^{*-}$ signal (full) are added.

and 4.9 mm, contributing with 71%, 25% and 4%. The systematic error on the B^0 lifetime from the resolution function was estimated by neglecting the third gaussian and by adding an offset of $\pm 500\mu$m to the resolution function (see table 6).

The invariant $\pi_B^+\pi_D^-$ mass for the selected candidates is shown in figure 6. The lifetime was determined from candidates in the mass region 1 GeV/c^2 $< M_{\pi_B^+\pi_D^-} <$ 1.5 GeV/c^2. The combinatorial background fraction in the lifetime fit was constrained to the amount obtained as below from the mass spectrum. The sample consists of events where the π_D^- and π_B^+ originate from a $B \to \pi_B^+ X D^{*-} \to \pi_B^+ X (\pi_D^- \overline{D}^0)_{D^{*-}}$ decay and of combinatorial background.

- $B \to \pi_B^+ D^{*-} X$ **events**

  - B^0 **Signal.**
    The expected composition of the $B^0 \to \pi_B^+ X D^{*-} \to \pi_B^+ X (\pi_D^- \overline{D}^0)_{D^{*-}}$ sample in the signal mass region 1 GeV/c^2 $< M_{\pi_B^+\pi_D^-} <$ 1.5 GeV/c^2. is given in table 5. Branching ratios were taken from [18].
  - B^+ **background.**
    The amount of background from $B^+ \to \pi_B^+ X D^{*-}$ decays relative to the B^0 signal was estimated from a Monte Carlo simulation to be $B^+/(B^+ + B^0) = (8.3^{+2.3}_{-2.4})\%$ (see table 5). This ratio can be determined as well from a fit to the

Table 5: Expected number of events in the signal mass region 1 GeV/c^2 $< M_{\pi_B^+\pi_D^-} <$ 1.5 GeV/c^2. 275 events were observed in the data.

	# events expected				
$B^0 \to \pi_B^+ X D^{*-}$	57.3 $(\pi^+ D^{*-})$	44.5 $(\rho^+ D^{*-})$	40.7 $(X D^{*-})$	20.8 $(\pi^+, \rho^+ D^{**})$	163 ± 17
$B^+ \to \pi_B^+ X D^{*-}$	10.2 $(\pi^+ D^{**})$	2.2 $(\rho^+ D^{**})$	2.3 $(X D^{*-})$		$14.7^{+3.9}_{-4.0}$
$b\bar{b}$ background					83.4 ± 8.3
$q\bar{q}$ background					10.6 ± 3.3
Sum					272 ± 20

$\pi_B^+\pi_D^-$ mass spectrum ($B^+/B = 12 \pm 22\%$) or from the number of rejected B^+ candidates ($B^+/B = 3.2 \pm 5.6\%$). All estimates agree. For the lifetime fit the ratio from the Monte Carlo simulation was taken.

$$r_+ \equiv \frac{B^+}{B^+ + B^0} = (8.3^{+2.3}_{-2.4} \pm 4.1)\%$$

A systematic error of 50% was added to take into account uncertainties in the D^{**} production rate. $B^+ \to \pi^+, \rho^+ \overline{D^{**}}^0$ decays were simulated with relative rates according to [18] and normalized to the measured $B^+ \to \pi^+\pi^+ D^{*-}$ branching ratio [19].

- **Combinatorial background**.
  The combinatorial background was estimated from a Monte Carlo simulation. The $\pi_B^+\pi_D^-$ mass spectrum for this background in Monte Carlo events is shown in figure 6. The background spectrum was normalized to the data in the region $M_{\pi\pi} >$ 1.5 GeV/c^2 where $B \to \pi_B^+ X D^{*-} \to \pi_B^+ X \pi_D^- \overline{D}^0$ events cannot contribute. The number of background events $N_b = 94.0 \pm 9.6$ was obtained from an extrapolation to the signal mass region 1 GeV/c^2 $< M_{\pi_B^+\pi_D^-} <$ 1.5 GeV/c^2.

A background sample, consisting of three subsamples, was selected from data to describe the combinatorial background time distribution. The first subsample was selected from wrong charge combinations $\pi_B^\pm\pi_D^\pm$ applying the same selection criteria as for the signal sample. The fact that slow pions are distributed isotropically around the jet axis motivates the selection of the second subsample. The momentum of the slow pion was first rotated around the jet axis $\vec{p}_{\pi_D} \to \vec{p'}_{\pi_D}$ so that the momentum difference $|\vec{p}_{\pi_D} - \vec{p'}_{\pi_D}|$ is 200 MeV/c with a maximal rotation angle of $\pm 90°$. Then the normal selection was applied. The rotation with a momentum difference of 200 MeV/c is large enough to destroy the correlation between the π_B^+ and π_D^- in signal events. The third sample consists of wrong sign combinations with a rotation of the slow pion. The total background sample is the sum of the three subsamples.

5.2 B^0 lifetime measurement

The lifetime was determined with an unbinned maximum likelihood fit to the signal candidates and background events in the mass region 1 GeV/c^2 $< M_{\pi_B^+\pi_D^-} <$ 1.5 GeV/c^2. Six events, included in the analysis with fully reconstructed B^0 decays, and one event, reconstructed as semileptonic B^0 decay, were rejected. The likelihood is a function of the expected time distributions for the signal and for background events. The time distribution for the B^0 signal events is an exponential folded with resolution functions R^ℓ,R^p and the momentum distribution $g(p_t)$, taking into account the reconstruction efficiency $\epsilon(p_t, \ell_t)$.

$$\mathcal{P}_s(t) =$$
$$a_s \int_{30\ GeV/c}^{45\ GeV/c} dp \int dp_t \int d\ell_t \ \underbrace{R^\ell(\ell,\ell_t)\ R^p(p,p_t)}_{\text{resolution functions}}\ \underbrace{\epsilon(p_t,\ell_t)}_{\text{efficiency}}\ \underbrace{g(p_t)}_{\text{momentum spectrum}}\ \underbrace{\frac{1}{\tau}\ e^{-t_t/\tau}}_{\text{decay function}}$$

The true decay time t_t is related to true momentum p_t and true decay length ℓ_t by $t_t = \ell M_B/p_t c$. R^ℓ, R^p, g and ϵ were taken from simulated events with a Peterson fragmentation parameter ϵ_b set to the measured value of $\epsilon_b = 0.0032 \pm 0.0017$ [20]. A normalization factor a_s guarantees $\int_{1\ ps}^{20\ ps} dt\ \mathcal{P}(t) = 1$.

For the time distribution of $B^+ \to \pi^+ X D^{*-}$ decays a normalized exponential with an effective B^+ lifetime was taken.

$$\mathcal{P}_+(t) = \exp(t, \tau_+^{eff}) \equiv \frac{1}{\tau_+^{eff}} \cdot \left(e^{-1\ ps/\tau_+^{eff}} - e^{-20\ ps/\tau_+^{eff}} \right)^{-1} \cdot e^{-t/\tau_+^{eff}}$$

The effective lifetime of $\tau_+^{eff} = 1.01 \pm 0.17$ ps was obtained from a simulation using the world average B^+ lifetime $\tau_+ = 1.67 \pm 0.08$ ps [21]. The error on τ_+^{eff} is the statistical error from the simulation. Varying the B^+ lifetime within the errors led to an uncertainty which was included in the systematic error on the B^0 lifetime (see table 6).

The combinatorial background was described by a sum of two normalized exponentials.

$$\mathcal{P}_b(t) = r_b \cdot \exp(t, \tau_{b1}) + (1 - r_b) \exp(t, \tau_{b2})$$

The likelihood function is a product for the signal sample and the background sample:

$$\mathcal{L} = \mathcal{L}^{signal}(\tau;\ r_+, N_s, N_b, r_b, \tau_{b1}, \tau_{b2}, \tau_+^{eff}) \cdot \mathcal{L}^{backg}(r_b, \tau_{b1}, \tau_{b2})$$

with eight fit parameters:

$\boldsymbol{\tau}$	: B^0 lifetime
$\boldsymbol{N_s}$	: Number of events $B^0, B^+ \to \pi_B^+\ X\ (D^0\pi_D^-)_{D^*}$.
$\boldsymbol{N_b}$	: Number of background events ($< N_b >= 94.0 \pm 9.6$).
$\boldsymbol{r_+}$	: relative amount of B^+ background, constrained to $< r_+ >= 8.3 \pm 4.8\%$.
$\boldsymbol{r_b}$, $\boldsymbol{\tau_{b1}}$, $\boldsymbol{\tau_{b2}}$	: parameters to describe the background time spectrum.
$\boldsymbol{\tau_+^{eff}}$	: the effective lifetime for the B^+ background ($< \tau_+^{eff} >= 1.01 \pm 0.17$ ps).

The likelihood for the signal part includes the constraints on N_b, τ_+ and r_+.

$$\mathcal{L}^{signal} = e^{-\frac{(N_b - <N_b>)^2}{2\sigma^2_{N_b}}} \cdot e^{-\frac{(r_+ - <r_+>)^2}{2\sigma^2_{r_+}}} \cdot e^{-\frac{(\tau_+ - <\tau_+>)^2}{2\sigma^2_{\tau_+}}} \cdot e^{-N_s - N_b} \cdot \prod_{i}^{\substack{signal \\ sample}} \mathcal{P}_i$$

with

$$\mathcal{P}_i = N_s \left[(1 - r_+)\mathcal{P}_{s,i} + r_+ \mathcal{P}_{+,i}\right] + N_b \mathcal{P}_{b,i}$$

The likelihood for the background sample only depends on the parameters r_b, τ_{b1} and τ_{b2}:

$$\mathcal{L}^{backg} = \prod_{i}^{\substack{background \\ sample}} \mathcal{P}_{b,i}$$

Figure 7 shows the proper time spectrum for the signal and background samples together with the fit result. The lifetime was determined to be

$$\tau_0 = 1.49 \, ^{+0.17}_{-0.15} \, ^{+0.08}_{-0.06} \text{ ps}$$

The sources of systematic errors are given in table 6. The main error came from the uncertainty on the background time distribution. The assumption that the background sample describes the real background in the signal sample has been checked with Monte Carlo events and was found to valid within the statistical errors. The corresponding systematic error reflects the statistical error in the Monte Carlo simulation.

systematic error	
background time distribution	$^{+0.057}_{-0.044}$ *ps*
parametrization of $\mathcal{P}_+(t)$ and $\mathcal{P}_b(t)$	± 0.011 *ps*
momentum and decay length resolution	± 0.024 *ps*
efficiency (MC statistic)	$^{+0.037}_{-0.020}$ *ps*
efficiency (parametrization, signal composition)	± 0.019 *ps*
B^+ lifetime ($\tau_{B^+} = 1.67 \mp 0.08$ *ps*)	$^{+0.002}_{-0.005}$ *ps*
fragmentation function ($\epsilon_b = 0.0032 \pm 0.0017$)	$^{+0.006}_{-0.008}$ *ps*
sum	$^{+0.076}_{-0.059}$ *ps*

Table 6: Systematic uncertainties.

6 Conclusions

The lifetimes of the $\bar{B}^0$ and B^- mesons have been measured with the ALEPH detector at LEP, using three different methods. The method using $D^{(*)}\ell$ correlations yielded:

$$\tau_0 \;=\; 1.61 \pm 0.07 \pm 0.04 \text{ ps}$$

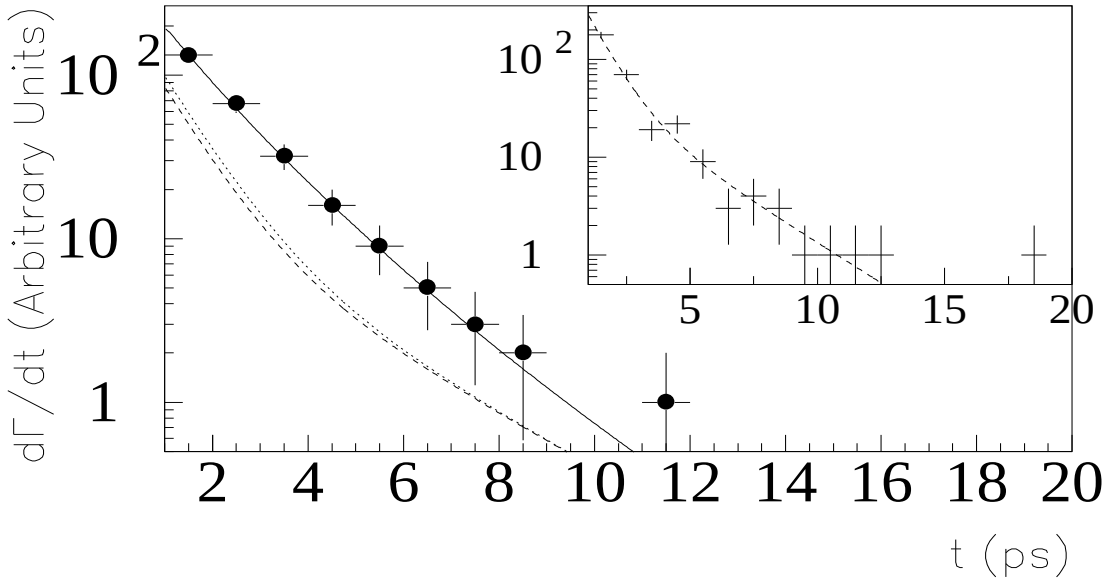

Figure 7: Fit results for the signal and the background sample. For the signal sample the dashed and dotted curve are the combinatorial background contribution and the total background, including $B^+ \to \pi^+ X D^{*-}$ decays.

$$\begin{aligned} \tau_- &= 1.58 \pm 0.09 \pm 0.04 \text{ ps} \\ \frac{\tau_-}{\tau_0} &= 0.98 \pm 0.08 \pm 0.02. \end{aligned}$$

A second method, using fully reconstructed hadronic $\bar{B}^0$ and B^- decays, obtained:

$$\begin{aligned} \tau_0 &= 1.25^{+0.15}_{-0.13} \pm 0.05 \text{ ps} \\ \tau_- &= 1.58^{+0.21}_{-0.18} \pm 0.04 \text{ ps} \\ \frac{\tau_-}{\tau_0} &= 1.27^{+0.23}_{-0.19} \pm 0.03. \end{aligned}$$

Finally, a method that uses a partial reconstruction technique to identify $\bar{B}^0 \to D^{*+}\pi^- X$ decays gave the result:

$$\tau_0 = 1.49^{+0.17+0.08}_{-0.15-0.06}$$

All these results are preliminary.

Events that were selected by more than one analysis were retained only once, such that the three measurements are statistically independent. A total of eight events were removed in this way. Furthermore, the different nature of the three analyses leads to independent systematic uncertainties. Therefore a simple weighted average was used to combine the results.

The combined preliminary results are:

$$\tau_0 = 1.54 \pm 0.07 \text{ ps}$$

$$\begin{aligned} \tau_- &= 1.58 \pm 0.09 \text{ ps} \\ \frac{\tau_-}{\tau_0} &= 1.02 \pm 0.08 \end{aligned}$$

7 Acknowledgments

We thank our colleagues in the accelerator divisions for the continued good performance of LEP. Thanks also to the many engineering and technical personnel at CERN and at the home institutes for their contributions to the performance of the ALEPH detector. Those of us from non-member states thank CERN for its hospitality.

References

[1] B. Buskulic, *et al.* (ALEPH Collab.), Phys. Lett. B **307** (1993) 194.

[2] ALEPH Collab., "Measurement of the B^- and $\bar{B}^0$ lifetimes using exclusively reconstructed events,"contributed paper to *XXVII International Conference on High Energy Physics, July 1994, Glasgow,* GLS620.

[3] D. Decamp *et al.* (ALEPH Collaboration), Nucl. Instrum. Methods A **294** (1990) 121.

[4] G. Batignani *et al.*, "Recent Results and Running Experience of the New ALEPH Vertex Detector", Conference Record of the 1991 IEEE Nuclear Science Symposium, November 2-9, 1991, Santa Fe, New Mexico, USA.

[5] D. Buskulic *et al.*, (ALEPH Collaboration), Nucl. Instr. Meth. A 360 (1995) 481.

[6] D. Buskulic *et al.*, (ALEPH Collaboration), Nucl. Instr. Meth. A 346 (1994) 461.

[7] B. Buskulic, *et al.* (ALEPH Collab.), Phys. Lett. B **294** (1992) 145.

[8] D. Buskulic *et al.*, (ALEPH Collaboration), Phys. Lett. B 313 (1993) 535.

[9] D. Buskulic *et al.*, (ALEPH Collaboration), "Measurement of the effective b quark fragmentation function at the Z^0 resonance," in preparation.

[10] D. Bortoletto, *et al.* (CLEO Collab.), Phys. Rev. Lett. **64** (1990) 2117.
H. Albrecht, *et al.* (ARGUS Collab.), Z. Phys. C. **54** (1992) 1.

[11] ALEPH Collab., "Measurement of the B^- and $\bar{B}^0$ meson lifetimes," contributed paper to *XXVII International Conference on High Energy Physics, July 1994, Glasgow,* GLS0578.

[12] Particle Data Group, Phys. Rev. D50 (1994) 1173.

[13] H. Albrecht, *et al.* (ARGUS Collab.), Phys. Lett. B324 (1994) 249.

[14] B. Barish, *et al.* (CLEO Collab.), CLNS-94-1985.
H. Albrecht, *et al.* (ARGUS Collab.), Z. Phys. C57 (1993) 553.

[15] D. Buskulic *et al.*, (ALEPH Collaboration), Phys. Lett. B 345 (1994) 103.

[16] M. Athanas, *et al.* (CLEO Collab.), CLNS-94-1286.

[17] S. Bethke *et al* (JADE Collaboration), Phys. Lett. **B 213** (1988) 235.

[18] M.S. Alam *et al* (CLEO Collaboration), CLNS 94/1270 (1994).
C. Bebek *et al* (CLEO Collaboration), Phys. Rev. **D36** (1987) 1289.
A.Albrecht *et al* (ARGUS Collaboration), Z. Phys. **C48** (1990) 543.
Bortoletto *et al* (CLEO Collaboration), Phys. Rev. **D45** (1992) 21.

[19] P. Colangelo, F. De Fazio, G. Nardulli, Phys. Lett. **B303** (1993) 152. *a_1 and a_2 were set to* 1.15 *and* 0.26*, respectively.*

[20] D. Buskulic *et al* (ALEPH Collaboration), Z. Phys. **C62** (1994) 179.

[21] R. Forty, "Lifetimes of Heavy Flavour Particles," proceedings of "Physics in Collision 14," ed. S. Keller and H. D. Wahl.